

# Autoregressive Synthesis of Sparse and Semi-Structured Mixed-Type Data

Thomas Rückstieß  
Independent Researcher  
Melbourne, Australia  
research@tomr.au

Robin Vujanic  
MongoDB  
Sydney, Australia  
robin.vujanic@mongodb.com

## ABSTRACT

Synthetic data generation is a critical capability for data sharing, privacy compliance, system benchmarking and test data provisioning. Existing methods assume dense, fixed-schema tabular data, yet this assumption is increasingly at odds with modern data systems—from document databases, REST APIs to data lakes—which store and exchange data in sparse, semi-structured formats like JSON. Applying existing tabular methods to such data requires flattening of nested data into wide, sparse tables which scales poorly. We present ORIGAMI, an autoregressive transformer-based architecture that tokenizes data records, including nested objects and variable length arrays, into sequences of key, value and structural tokens. This representation natively handles sparsity, mixed types and hierarchical structure without flattening or imputation. ORIGAMI outperforms baselines spanning GAN, VAE, diffusion and autoregressive architectures on fidelity, utility and detection metrics across nearly all settings, while maintaining high privacy scores. On semi-structured datasets with up to 38% sparsity, baseline synthesizers either fail to scale or degrade substantially, while ORIGAMI maintains high-fidelity synthesis that is harder to distinguish from real data. To the best of our knowledge, ORIGAMI is the first architecture capable of natively modeling and generating semi-structured data end-to-end.

### PVLDB Reference Format:

Thomas Rückstieß and Robin Vujanic. Autoregressive Synthesis of Sparse and Semi-Structured Mixed-Type Data. PVLDB, 14(1): XXX-XXX, 2020. doi:XX.XX/XXX.XX

### PVLDB Artifact Availability:

The source code, data, and/or other artifacts have been made available at <https://github.com/rueckstieess/origami-jsynth>.

## 1 INTRODUCTION

Synthetic data generation has become an important capability in modern data management. Organizations require realistic data for privacy-preserving data sharing, software testing, provisioning of development and QA environments, training of Machine Learning models and benchmarking database workloads at scale [14, 28]. Growing regulatory pressure, including GDPR, HIPAA, and sector-specific data governance mandates, has necessitated the ability to produce statistically faithful surrogates of sensitive datasets.

A rich body of work now addresses tabular data synthesis [30], spanning generative adversarial networks (GAN) and variational autoencoders (VAE) [20, 40], diffusion models [18, 29, 45], and autoregressive approaches [2, 6, 31, 35]. Despite this architectural diversity, one assumption has remained largely unchallenged: all methods operate on fixed-schema tables with dense, homogeneously typed columns, treating sparsity as a data issue that needs to be fixed during preprocessing. Approaches to tackle this sparsity range from mean imputation of missing numerics, sentinel values for categorical missingness, to dropping sparse rows entirely—in each case destroying structural properties of the data that we argue ought to be modeled.

This *dense table* assumption is increasingly at odds with a large and growing share of modern data workloads. While transactional systems continue to rely on relational schemas, application-layer data is overwhelmingly exchanged and often stored in semi-structured formats. Document databases, REST APIs, data lakes, and event streams operate on JSON records rather than flat tables [3, 5, 33]. A single business listing in a review platform, for instance, may contain nested objects for operating hours and location, variable-length arrays for categories and reviews, optional keys that differ across records, and even type polymorphism where the same key path holds an integer in one record and a string in another.

To apply existing data synthesis methods to semi-structured data, the only recourse is to first flatten nested structures into tables. But this transformation is problematic and scales poorly. Variable-length arrays produce sparse trailing columns, type-polymorphic keys require splitting into per-type sub-columns, and optional keys carry semantic meaning. In our experiments, flattening real-world JSON datasets produces tables with many hundreds of columns and sparsity exceeding 37%. These tables are qualitatively different from the dense 10–20 column benchmark datasets from the UCI repository [15] frequently found in the synthetic data generation literature, e.g. Adult (48K rows, 15 columns), Shoppers (12K rows, 18 columns), and Magic (19K rows, 11 columns).

A secondary tension concerns the treatment of mixed types. Methods that operate in continuous latent space (GANs, VAEs, diffusion models) handle numerics natively but must encode categorical columns, often through one-hot vectors that scale poorly with cardinality. This failure mode gets amplified in flattened semi-structured data, as array expansion inflates the categorical column count into the hundreds or thousands. On the other hand, autoregressive and LLM-based methods handle categoricals natively as tokens but must discretize high-cardinality numeric values to avoid vocabulary explosion, which sacrifices precision and ordinal structure.

This work is licensed under the Creative Commons BY-NC-ND 4.0 International License. Visit <https://creativecommons.org/licenses/by-nc-nd/4.0/> to view a copy of this license. For any use beyond those covered by this license, obtain permission by emailing [info@vldb.org](mailto:info@vldb.org). Copyright is held by the owner/author(s). Publication rights licensed to the VLDB Endowment.

Proceedings of the VLDB Endowment, Vol. 14, No. 1 ISSN 2150-8097.  
doi:XX.XX/XXX.XX

To address these issues, we present ORIGAMI (Object Representation via Generative Autoregressive ModellIng), an autoregressive transformer with a dual-head discrete/continuous architecture that operates directly on tokenized JSON records, avoiding flattening entirely. Our tokenization scheme serializes nested objects, arrays, and primitive values into sequences of key, value, and structural tokens, preserving hierarchy and sparsity as first-class properties of the data. Key-Value Position Encoding (KVPE) replaces the usual sequential position indices with structural path encodings derived from each token’s location in the document tree, making the model invariant to the order of sibling keys. This invariance enables key-order shuffling as a data augmentation strategy that prevents memorization by presenting each training record in a different key order at every epoch. The dual-head architecture predicts discrete tokens (keys, categorical values, and structural delimiters) through next-token prediction and continuous numeric values are modeled as parameterized Mixture of Gaussians, handling both data types in their native representation without discretization or one-hot encoding. Grammar and schema constraints, enforced via a pushdown automaton and a compiled mask table, guarantee that every generated record is syntactically valid JSON conforming to the learned data schema.

While ORIGAMI is primarily designed for semi-structured data modeling, it achieves excellent results on standard tabular benchmarks (representable in JSON as flat key-value pairs), exceeding state-of-the-art diffusion and autoregressive baselines across fidelity, detection, and utility metrics while retaining high privacy scores at or above 97%. On sparse and semi-structured datasets with up to 38% sparsity and over one million records, baseline synthesizers’ performance degrades substantially; ORIGAMI maintains high-fidelity synthesis that is harder to distinguish from real data.

Our contributions are as follows:

- (1) We introduce the first architecture, to our knowledge, capable of end-to-end synthesis of semi-structured data, natively handling hierarchical nesting, variable-length arrays, sparsity, and type polymorphism without flattening or imputation.
- (2) We propose Key-Value Position Encoding (KVPE) as a principled mechanism for order-invariant modeling of shuffled key-value data, and demonstrate its effectiveness as a regularizer against memorization.
- (3) We develop a flattening methodology and propose enhancements to standard evaluation metrics for semi-structured datasets that enables fair evaluation of ORIGAMI against tabular baselines, while also considering type fidelity and structural missingness patterns.
- (4) We evaluate on datasets ranging from academic tabular benchmarks to large-scale semi-structured collections with over one million records, demonstrating state-of-the-art results across nearly all settings.

Code to reproduce our experiments is available<sup>1</sup>. ORIGAMI is additionally published as an easy-to-use standalone Python package (`origami-ml`) under permissive MIT license with a Python SDK and CLI interface.

<sup>1</sup><https://github.com/rueckstiess/origami-jsynth>

## 2 RELATED WORK

*GAN and VAE-based Synthesis.* Generative Adversarial Networks [12] train a generator to produce synthetic samples that a co-trained discriminator cannot distinguish from real data. Variational Autoencoders [16] instead learn a regularized latent space from which new samples can be decoded, optimizing a lower bound on the data likelihood. Both paradigms have been adapted for tabular synthesis, most notably as CTGAN and TVAE [40]. Many variants have since been proposed [30], e.g. GOGGLE [20], which extends the VAE framework by replacing the MLP decoder with a Message Passing Neural Network over a jointly learned column dependency graph.

*Diffusion Synthesis.* Diffusion models generate data by learning to reverse a noise process that gradually corrupts real samples into Gaussian noise. TabDDPM [18] first applied diffusion to mixed-type tabular data via separate Gaussian and multinomial processes for numerical and categorical features. TabSyn [45] improved sampling speed and fidelity by performing diffusion in a VAE latent space, and TabDiff [29] further introduced feature-wise learnable noise schedules to adaptively allocate model capacity across heterogeneous columns, achieving state-of-the-art results on many standard benchmarks.

*Autoregressive Synthesis.* Autoregressive models decompose the joint distribution into a product of conditionals,  $p(x_1, \dots, x_n) = \prod_{i=1}^n p(x_i | x_1, \dots, x_{i-1})$ , generating one variable at a time. GReaT [2] and Tabby [6] fine-tune a pretrained GPT-2 [27] backbone on rows serialized as natural language, with Tabby adding a Mixture-of-Experts output head per column. REaLTabFormer [31] instead trains a GPT-2 architecture from scratch on a dataset-specific vocabulary with digit-level numerical encoding and constrained decoding. ORIGAMI’s approach is similar in that it also produces a dataset-specific vocabulary of keys and values, but additionally includes structural tokens to model hierarchy and nesting. TabularARGN [35] departs from transformers, adopting a lightweight NADE-inspired [36] architecture of per-column MLP regressors over discretized sub-columns. Several autoregressive methods randomly permute the factorization order during training as proposed by [1, 42], effectively learning an ensemble over all orderings to regularize against spurious correlations and enable arbitrary conditional generation at inference, which ORIGAMI employs as well.

While not specifically designed for data synthesis, [11] adds a second continuous head to the standard LLM architecture, making it a hybrid discrete/continuous model. We adopt this approach in ORIGAMI, however instead training with MSE loss for single scalar regression, we model continuous values as a Mixture of Gaussians and train with a negative log likelihood loss to better adapt to uncertainty and multi-modal distributions. For constrained decoding, we extend ideas from [17, 38], applying grammar and schema constraints during both training and inference to accelerate convergence and enforce valid token sequences.

*Synthesis beyond Single Tables.* The database community has explored synthetic data generation for benchmarking and privacy-preserving data sharing. SAM [41] uses supervised autoregressive models to generate databases satisfying cardinality constraints from query workloads, and PrivBench [10] synthesizes benchmark databases that preserve both data distributions and query runtime

characteristics under differential privacy (DP). For multi-table settings, PrivLava [4] introduces graphical models with latent variables to capture inter-table correlations under DP, and REaLTabFormer [31] extends its single-table transformer with a Seq2Seq model for parent-child table relationships. All of these methods assume relational schemas with fixed-width rows; none operate on semi-structured records with variable nesting or optional keys.

*Sparsity and Missing Data.* Most tabular synthesizers assume fully observed inputs and handle missingness through imputation or row dropping. [22] formalize DP synthetic data generation when inputs contain missing values, proposing adaptive strategies that improve utility by modeling missingness patterns rather than imputing them away. In scientific computing, Sparse Data Diffusion [23] explicitly encodes exact zeros through auxiliary “sparsity bits” rather than treating them as continuous values, recognizing that sparsity carries semantic information. Both works identify the need to model sparsity as a first-class property of the data, but neither extends to the hierarchical, variable-schema setting that characterizes semi-structured data.

### 3 ARCHITECTURE

ORIGAMI falls into the category of autoregressive transformer-based methods. Unlike previous work, which assumes flat tabular inputs, it operates on tokenized representations of JSON records. We describe each component in turn: preprocessing, tokenization, the model architecture including Key-Value Position Encoding (KVPE), output heads, grammar and schema constraints and post-processing of numeric data.

Throughout this work, we use standard tabular terminology, *rows* and *columns*, when referring to flat table representations. For semi-structured data, we use *records* (analogous to rows) and *keys* (analogous to columns), to refer to the entries and named attributes of a JSON record. A *key path* is the dot-separated concatenation of nested keys through the record tree, with integer indices for array positions: for example, `user.addresses.0.city` refers to the `city` key of the first element in the `addresses` array under the `user` key.

#### 3.1 Preprocessing

Numeric keys in semi-structured data span a wide range of cardinalities. Low-cardinality keys (e.g., a `rating` key with integers 1–5) are treated as categorical tokens. For high-cardinality numeric keys (more than  $\tau$  distinct values, where  $\tau$  is a configurable threshold), we apply per-key standardization. Let  $x$  be a value of key  $k$ ; we compute

$$\hat{x} = \frac{x - \mu_k}{\sigma_k}, \quad (1)$$

where  $\mu_k$  and  $\sigma_k$  are the mean and standard deviation of numeric values under key  $k$  estimated from training data. Scaled values are passed to the model through a dedicated continuous channel described in Section 3.5 and inverse-transformed during post-processing (Section 3.9).

#### 3.2 Tokenization

Our tokenization scheme differs from typical tokenizers used in the language modeling literature, such as Byte-pair Encoding [9] and WordPiece [39], in that we tokenize JSON instances into key

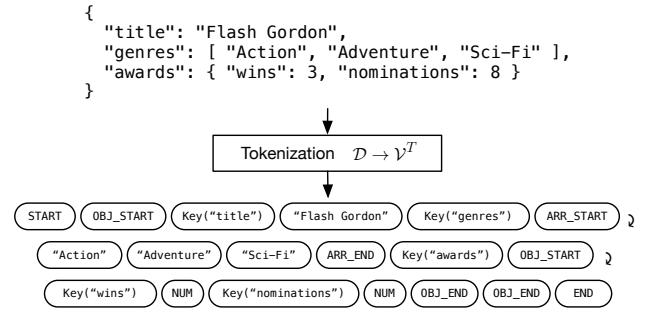


Figure 1: Tokenization of an example *movies* record.

and value tokens and maintain the structure of arrays and nested objects with special grammatical tokens.

For a dataset  $\mathcal{D}$ , each JSON record  $d \in \mathcal{D}$  is serialized into a token sequence  $\mathbf{x} = (x_1, \dots, x_T)$  by a depth-first traversal. The vocabulary  $\mathcal{V}$  consists of three disjoint token classes,  $\mathcal{V} = \mathcal{V}_s \cup \mathcal{V}_k \cup \mathcal{V}_v$  as follows:

- **Structural tokens**  $\mathcal{V}_s = \{\text{START, END, OBJ\_START, OBJ\_END, ARR\_START, ARR\_END, PAD, NUM}\}$ , which delimit record boundaries, objects, arrays and a sentinel NUM placeholder when continuous modeling is enabled.
- **Key tokens**  $\mathcal{V}_k$ , one per distinct key observed in training.
- **Value tokens**  $\mathcal{V}_v$ , one per distinct categorical value (strings, booleans, null, and low-cardinality numbers).

Nested objects and arrays are handled recursively: an object value emits OBJ\_START . . . OBJ\_END, and an array emits ARR\_START . . . ARR\_END with its elements in order.

High-cardinality numeric values that were standardized in preprocessing (Section 3.1) emit a special NUM token in the discrete sequence, with the scaled value  $\hat{x}$  stored in a parallel continuous channel to train the continuous head (Section 3.5).

Alongside each token  $x_t$ , the tokenizer records its key path  $\mathbf{p}_t = (e_1, \dots, e_{D_t})$  through the JSON hierarchy, where each element  $e_i$  is either a key name or an array index, and  $D_t$  is the nesting depth. For instance, in `{"user": {"name": "Alice"}}`, the token for value Alice has path `(Key(user), Key(name))`.

Figure 1 illustrates the tokenization of an example JSON record.

#### 3.3 Input Representation

The input to the transformer at position  $t$  is the sum of a token embedding and a position embedding:

$$\mathbf{h}_t^{(0)} = \mathbf{e}(x_t) + \text{KVPE}(\mathbf{p}_t), \quad (2)$$

where  $\mathbf{e} : \mathcal{V} \rightarrow \mathbb{R}^d$  is a learned token embedding.

*Key-Value Position Encoding (KVPE).* Standard transformers typically use sequential, sinusoidal [37] or rotary [34] position indices. Since JSON key-value pairs have no inherent order, these positions would impose a spurious ordering on sibling keys. Instead, KVPE encodes each token’s *structural position* representing its path through the record tree.

Each path element is embedded independently: key elements reuse the token embedding matrix  $\mathbf{e}$  (tying key representations across the position and content channels), while array index elements use a separate embedding table  $\mathbf{e}_{\text{id}x} : \{0, \dots, I_{\text{max}}\} \rightarrow \mathbb{R}^d$ , where  $I_{\text{max}}$  is a fixed, configurable capacity for array position embeddings. The sequence of element embeddings  $(\mathbf{e}(e_1), \dots, \mathbf{e}(e_{D_t}))$  is aggregated into a single position vector via sum pooling:  $\text{KVPE}(\mathbf{p}_t) = \sum_{i=1}^{D_t} \mathbf{e}(e_i)$ .

*Numeric embedding.* For positions where  $x_t = \text{NUM}$ , we follow the approach in [11] and replace the token embedding  $\mathbf{e}(x_t)$  with a multiplicative embedding  $\tilde{x}_t \cdot \mathbf{v}_{\text{num}}$ , where  $\mathbf{v}_{\text{num}} \in \mathbb{R}^d$  is a learned direction vector and  $\tilde{x}_t$  is the standardized value. This injects continuous numeric information directly into the representation, encoding both the sign and magnitude of the standardized value as the direction and norm of the embedding vector.

### 3.4 Transformer Backbone

The backbone is a stack of  $L$  pre-norm decoder-only transformer layers with causal (autoregressive) attention:

$$\mathbf{z}_t^{(\ell)} = \mathbf{h}_t^{(\ell)} + \text{MHA}(\text{LN}(\mathbf{h}_t^{(\ell)})), \quad (3)$$

$$\mathbf{h}_t^{(\ell+1)} = \mathbf{z}_t^{(\ell)} + \text{FFN}(\text{LN}(\mathbf{z}_t^{(\ell)})), \quad (4)$$

where MHA is multi-head attention with  $H$  heads and head dimension  $d/H$ , FFN is a two-layer feed-forward network with GELU [13] activation and hidden dimension  $d_{\text{ff}}$ , and LN denotes layer normalization. A final layer norm is applied after the last layer. Causal masking ensures each position attends only to itself and earlier positions.

*Left-padding.* Since JSON records vary in length, batches are *left-padded* so that all sequences end at the same position. This allows  $\mathbf{h}_T^{(L)}$  to always be the representation of the last real token, simplifying batched next-token prediction.

### 3.5 Output Heads

The model has two output heads, inspired by [11]: a discrete head for structural, key, and categorical value tokens, and an optional continuous head for numeric values, as shown in Figure 2.

*Discrete head.* A linear projection maps the final hidden state to vocabulary logits:

$$\ell_t = \mathbf{W}_d \mathbf{h}_t^{(L)} + \mathbf{b}_d \in \mathbb{R}^{|\mathcal{V}|}, \quad (5)$$

trained with cross-entropy loss over all non-padding positions.

*Continuous head (Mixture of Gaussians).* For high-cardinality numeric keys, the discrete head emits a NUM token while a parallel continuous head models the numeric value. The continuous head projects the hidden state to parameters of a Mixture of Gaussians (MoG) with  $K$  components:

$$(\boldsymbol{\pi}_t, \boldsymbol{\mu}_t, \log \boldsymbol{\sigma}_t^2) = \text{split}(\mathbf{W}_c \mathbf{h}_t^{(L)} + \mathbf{b}_c) \in \mathbb{R}^{3K}, \quad (6)$$

where  $\boldsymbol{\pi}_t = \text{softmax}(\cdot)$  are mixture weights. The numeric value  $\tilde{x}_{t+1}$  is modeled as:

$$p(\tilde{x}_{t+1} | \mathbf{h}_t^{(L)}) = \sum_{j=1}^K \pi_{t,j} \mathcal{N}(\tilde{x}_{t+1}; \mu_{t,j}, \sigma_{t,j}^2). \quad (7)$$

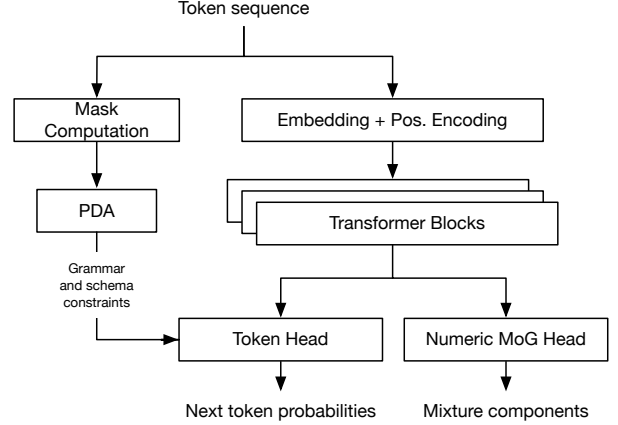


**Figure 2: ORIGAMI dual-head model architecture with grammar and schema constraints imposed on the discrete head.**

The continuous loss is the negative log-likelihood over positions where the target is a NUM token. The total training loss is:

$$\mathcal{L} = \mathcal{L}_{\text{CE}} + \lambda \mathcal{L}_{\text{NLL}}, \quad (8)$$

where  $\lambda$  is set proportionally to the fraction of NUM tokens to total tokens in each batch.

### 3.6 Key-Order Shuffling

Since JSON object keys are unordered by specification, we randomly permute the key order at each nesting level every time a training example is accessed. Combined with KVPE (which encodes structural position rather than sequential position), this augmentation forces the model to attend to key semantics rather than memorizing a canonical ordering. We demonstrate through ablation (see Section 5 and Figures 5 and 6) that this approach helps distinguish robust causal relationships from spurious correlations, as truly meaningful dependencies will persist across different ordering permutations, while coincidental correlations tend to average out during training. This mechanism also serves as an implicit regularization strategy similar to Dropout [32], as the model must learn to predict from varying subsets of conditioning variables. However, unlike Dropout where a portion of the gradient information is discarded, the order-agnostic approach maintains full use of the training signal.

### 3.7 Grammar Constraints

To guarantee syntactically valid JSON output, we employ a push-down automaton (PDA) that tracks the grammatical state during both training and generation. The PDA maintains a stack encoding the current nesting context (object vs. array at each depth level) along with flags for parser state (e.g., whether a key is awaiting its value).

At each position  $t$ , the PDA computes a boolean mask  $\mathbf{m}_t \in \{0, 1\}^{|\mathcal{V}|}$  indicating which tokens are grammatically valid as the

next token. Invalid token logits are set to  $-\infty$  before the softmax:

$$\hat{\ell}_{t,v} = \begin{cases} \ell_{t,v} & \text{if } m_{t,v} = 1, \\ -\infty & \text{otherwise.} \end{cases} \quad (9)$$

During training, grammar masks are computed in parallel across all positions. Since the PDA state updates involve many small sequential operations that incur synchronization overhead on GPU, mask computation is offloaded to CPU workers in the data loading pipeline: while the GPU executes forward and backward passes on the current batch, DataLoader workers prepare grammar masks for subsequent batches in parallel, hiding the constraint computation cost behind GPU-bound training. During autoregressive generation, the PDA state is updated incrementally in  $O(1)$  per step.

### 3.8 Schema Constraints

The grammar PDA (Section 3.7) enforces syntactic validity but says nothing about the *semantic* structure of the data: which keys may appear, what types each key admits, or which values are legal. To enforce these constraints, we derive a JSON Schema [26] (draft 2020-12 subset) from the training data and compile it into a schema mask that is intersected with the grammar mask at every decoding position.

*Schema derivation.* Given a training corpus  $\mathcal{D}$ , we automatically derive a JSON Schema by analyzing the data structure:

- **Types:** Each key’s observed Python types are mapped to JSON Schema types (string, integer, number, boolean, null, object, array).
- **Enumerations:** Keys with at most  $\tau$  distinct primitive values receive an enum constraint listing all observed values.
- **Key restrictions:** Object schemas set `additionalProperties: false`, restricting keys to those observed in training. Keys present in every object are marked `required`.
- **Array bounds:** Observed array lengths yield `minItems` and `maxItems` constraints. Arrays where all observed instances contain unique elements are marked `uniqueItems`.
- **Numeric bounds:** Observed minimum and maximum values are recorded per numeric key.

When the continuous numeric mode is active, the schema is transformed to reflect the preprocessed representation: enum values for scaled keys are removed (since numeric values are now continuous) and bounds are mapped to the standardized scale.

*Compiled mask table.* The schema is compiled into a mask table  $\mathbf{M} \in \{0, 1\}^{(P+1) \times |V|}$ , where  $P$  is the number of unique key paths. Row 0 is all-ones (the default for positions outside the schema, such as record delimiters); each subsequent row  $i$  is a boolean mask reflecting the type, enum, and key restrictions for key path  $i$ . Each token position  $t$  in the JSON tree maps to a key path via its KVPE path  $\mathbf{p}_{t+1}$  (with array indices replaced by a wildcard `*`). The schema mask for the full sequence is produced by mapping each position’s path to its schema table row and performing a single gather operation. The effective constraint mask is the intersection of grammar and schema masks:  $\hat{\mathbf{m}}_t = \mathbf{m}_t \wedge \mathbf{s}_t$ .

This design separates *path-dependent* constraints (type, enum, allowed keys), which are pre-computed and applied via a single

tensor gather at  $O(1)$  cost per position, from *count-dependent* constraints (`minItems`, `maxItems`, `required`, `uniqueItems`), which require tracking state during generation and are enforced incrementally at inference time only for performance reasons.

### 3.9 Post-Processing

Numeric preprocessing (Section 3.2) introduces artifacts: standardized values decoded through the continuous head may not lie on the original scale’s natural grid (e.g., integer keys produce floats, and sampled values may fall outside observed bounds). We apply a deterministic post-processing pass to each generated value using the *original-data* schema (before preprocessing transforms):

- (1) **Clip to bounds:** Enforce the key’s observed minimum and maximum.
- (2) **Snap to enum:** If the key has an enum constraint, replace the value with the nearest observed value for that key by absolute difference.
- (3) **Round to integer:** If the key type is `integer` and no enum applies, round to the nearest integer.

This pipeline is applied recursively to nested objects and arrays. Post-processing is a lightweight operation that does not require model inference, and ensures generated data conforms to the original data’s type and domain constraints.

## 4 EXPERIMENTS

ORIGAMI is evaluated against six tabular baseline synthesizers on five datasets spanning dense tabular benchmarks to large-scale semi-structured collections. We emphasize that the comparison on semi-structured datasets is not between architectures in isolation, but between two paradigms: flatten-then-synthesize versus native semi-structured generation. The flattening pipeline (Section 4.1) represents a reasonable approach for applying existing methods to semi-structured data, as any practitioner facing this problem today would need to perform a similar transformation.

Section 4.1 describes how we flatten and type-separate semi-structured data to enable baseline training and consistent evaluation. We then introduce the datasets (Section 4.2), describe the experiment protocol (Section 4.3) and evaluation metrics (Section 4.4), and detail per-model training configurations (Section 4.5).

### 4.1 Tabular Representation of Semi-Structured Data

Existing tabular synthesizers and evaluation metrics require fixed-schema tables. We apply a two-stage transformation to native JSON data to produce a flat table with homogeneously typed columns suitable for both baseline training and metric computation. The transformation is illustrated in Figure 3.

*Flattening.* Each JSON record is traversed depth-first. Nested keys are concatenated with dot separators to form column names: key “name” inside object “user” becomes column “user.name”. Array elements are indexed numerically: “tags.0”, “tags.1”, etc. Only leaf values (primitives and nulls) are retained. Since arrays vary in length across records, shorter instances produce NaN entries in trailing index columns. The resulting table has one column per unique leaf key path observed in the dataset. For datasets without

```

{"title": "Flash Gordon", "genres": ["Action", "Adventure", "Sci-Fi"], "awards": {"wins": 3, "nominations": 8}}
{"title": "Tron", "genres": ["Action", "Sci-Fi"], "awards": {"wins": "unknown"}}

```

↓ FLATTEN

title	genres.0	genres.1	genres.2	awards.wins	awards.nominations
Flash Gordon	Action	Adventure	Sci-Fi	3	8
Tron	Action	Sci-Fi	NaN	"unknown"	NaN

↓ SEPARATE TYPES

title	genres.0	genres.1	genres.2		awards.wins			awards.nominations	
			.dtype	.cat	.dtype	.num	.cat	.dtype	.num
Flash Gordon	Action	Adventure	cat	Sci-Fi	num	3	NaN	num	8
Tron	Action	Sci-Fi	missing	NaN	cat	NaN	unknown	missing	NaN

**Figure 3: Flattening and type separation of two movie records. Nested objects and arrays are mapped to dot-separated columns; variable-length arrays and absent keys produce NaN. Mixed-type columns (awards.wins: integer vs. string) and partially-present columns are expanded into a type indicator (.dtype) and per-type value columns. Homogeneous, fully-present columns (title, genres.0, genres.1) pass through unchanged.**

nested key paths or arrays, flattening produces the original table unchanged.

*Type separation.* After flattening, a single column may contain values of different types across rows, or be absent from some records entirely (NaN). Such columns are expanded into typed sub-columns: a categorical indicator column “col.dtype” records the per-row type (num, cat, bool, null, or missing), and a separate column per observed type (“col.num”, “col.cat”, “col.bool”) holds the cast value, with NaN in rows of other types. This preserves the distinction between explicit null values (key present with value null) and structurally absent keys (key not present in the record). The explicit modeling of missing values via the .dtype column also allows tabular synthesizers to produce missing values during generation, even if not natively supported.

For baseline training, type separation is applied selectively: columns that are already homogeneous and fully present are kept as single columns to avoid unnecessary expansion. For evaluation, type separation is applied to all columns unconditionally and includes an additional “col.len” column for arrays, tracking their lengths explicitly, so that type fidelity and structural patterns can be measured directly.

*Application.* Baseline synthesizers train on the flattened, type-separated table. The transformation is then inverted to reconstruct JSON records. The same flattening and type separation is applied jointly to real and synthetic records during evaluation, ensuring a consistent column schema for all metrics. For tabular datasets, flattening is a no-op and type separation only activates for columns that require it, so the transformation reduces to the identity for dense, single-type columns.

## 4.2 Datasets

We evaluate all baselines on 5 datasets with varying size, categorical complexity and sparsity: Adult, Diabetes, Electric Vehicles, Yelp and DDXPlus.

*Adult and Diabetes.* These two datasets were chosen as the two largest datasets evaluated in TabDiff [29]. They originally stem from the UCI Machine Learning Repository [15]. We use TabDiff’s exact preprocessing code and splits for reproducibility and to establish a baseline. We note that TabDiff’s preprocessing of the Diabetes datasets consolidates empty strings (“”), question marks (“?”) and single spaces (“ ”) into a single nan value and uses an Ordinal Encoder from scikit-learn [25] to process the age column. While ORIGAMI technically doesn’t require this preprocessing, nevertheless we follow this approach for the Diabetes dataset. For evaluating ML utility, we predict income on the Adult dataset and readmitted on Diabetes.

*Electric Vehicles.* This tabular dataset contains 210,011 electric vehicle registrations from the New York State Department of Motor Vehicles<sup>2</sup>. We remove two degenerate columns (VIN is unique and Fuel Type is constant across all records) and convert date columns to Unix epoch integers. Several numeric keys (Unladen Weight, Maximum Gross Weight, Passengers) are structurally sparse—absent for vehicle subtypes where they do not apply—yielding 11% total sparsity. The utility target is Body Type.

*Yelp.* This JSON-native dataset contains 150,346 business records from the Yelp Open Dataset<sup>3</sup>. We remove unique identifier keys and split the comma-separated categories string into an array. Each record contains nested objects for business attributes (up to 39 optional keys) and operating hours, plus a variable-length category array. The attributes object is the primary source of structural sparsity, varying widely across business types. After flattening, the dataset expands to 266 columns with 38% sparsity. The utility target is is\_open.

<sup>2</sup>Snapshot obtained on 2026-02-12 from <https://data.ny.gov/Transportation/Electric-Vehicle-Registrations/3vp6-cxmr>

<sup>3</sup>Data obtained from <https://www.yelp.com/dataset>

**Table 1: Dataset characteristics after flattening and separating types into homogeneous columns**

Dataset	Records	#Num	#Cat	Total Cat.	Sparsity
Adult	32,561	6	9	104	0.0%
Diabetes	61,059	13	24	2,157	0.0%
Electric Vehicles	210,011	5	13	6,678	11.1%
Yelp	150,346	5	261	27,090	37.8%
DDXPlus	1,025,602	50	144	6,705	34.6%

*DDXPlus*. DDXPlus [8] is a large-scale medical diagnosis JSON dataset from the NeurIPS 2022 Datasets and Benchmarks track. The data was synthetically generated from a validated medical knowledge base, producing deterministic symptom–diagnosis relationships, which explains the near-perfect classification scores observed in the utility metric (Table 4) and makes the dataset valuable primarily as a stress test for structural complexity and scale rather than classification difficulty. Each of the 1,025,602 records contains demographics, a pathology label (49 classes, our utility target), and two variable-length arrays: symptom evidences and differential diagnoses with associated probabilities. After flattening, the dataset expands to 230 columns with 34.6% sparsity. At over one million records, DDXPlus is the largest dataset in our benchmark.

Table 1 summarizes the dataset characteristics after flattening and type separation. Sparsity denotes the fraction of structurally absent cells (key not present in the record), as opposed to explicit nulls.

### 4.3 Experiment Protocol

*Data splits*. For Adult and Diabetes, we use the exact preprocessing and train/test splits provided by TabDiff [29] to ensure a direct comparison. For Electric Vehicles, Yelp, and DDXPlus, we split 80/10/10 into train, validation, and test sets. Hyperparameter selection for ORIGAMI uses the inner train/validation split; final evaluation uses the full training set and held-out test set. The privacy metrics evaluation requires different split proportions, which is explained in Section 4.4.

*Training*. All training runs were conducted on a single NVIDIA V100 (16GB) GPU with a maximum wall-clock budget of 24 hours per run. Unless stated otherwise, we use the default hyperparameter configurations reported in each model’s original publication. We made every effort to train each model on all datasets; for the largest datasets (Yelp and DDXPlus), some models required reduced batch sizes and disabled costly validation-set evaluation during training. Details for each model can be found in Section 4.5.

*Sampling*. For each trained model, we generate 10 replicate sample sets with different random seeds matching the size of the training split. Each sample set is evaluated individually against fidelity, utility, detection and privacy metrics. We average all scores and report mean and standard deviation across replicates in Tables 3, 4, 5 and 6.

### 4.4 Evaluation Metrics

We evaluate synthetic data along four dimensions: *fidelity*, *utility*, *detection*, and *privacy*. All primary scores are normalized to  $[0, 1]$  with 1.0 being best. Standard tabular evaluation metrics (e.g., SDMetrics [7]) assume flat tables with single-type columns and silently drop missing values. This makes them unsuitable for semi-structured data where keys may be variably present, heterogeneously typed, or structurally nested. We therefore extend the standard metrics with modifications that explicitly account for structural missingness and type polymorphism. All metrics operate on the flattened, type-separated representation (Section 4.1), ensuring a consistent column schema across synthesizers, including ORIGAMI. By design, our modified metrics collapse to the standard metrics (e.g. provided by the SDMetrics package) for dense, homogeneous tables.

*Fidelity*. Fidelity measures how well synthetic data reproduces the statistical properties of the training data. The overall fidelity score is the average of two sub-scores: Column Shapes (marginal distributions) and Column Pair Trends (pairwise dependencies).

For *Column Shapes*, standard practice computes a single similarity statistic per column—Kolmogorov–Smirnov (KS) Complement for numeric columns, Total Variation (TV) Complement for categorical columns—and averages across columns. This fails on type-separated data: a column like `awards.wins.num` may be NaN in rows where the key is absent or holds a non-numeric type, and simply dropping these rows conflates structural absence with distributional similarity.

We instead decompose the per-column joint distribution over presence, type, and value via the chain rule, and measure real-vs-synthetic similarity at each factor independently for every column:

$$\varphi_{\text{pres}}(c) = \text{sim}(P_r(\text{Pres} | c), P_s(\text{Pres} | c)) \quad (10)$$

$$\varphi_{\text{type}}(c) = \text{sim}(P_r(T | c, \text{pres}), P_s(T | c, \text{pres})) \quad (11)$$

$$\varphi_{\text{val}}(c) = \text{sim}(P_r(V | c, \text{pres}, T), P_s(V | c, \text{pres}, T)) \quad (12)$$

where  $P_r$  and  $P_s$  denote the real and synthetic distributions for given column  $c$ ,  $\text{sim}$  is TV Complement for discrete distributions and KS Complement for continuous ones, and each factor conditions on the previous level. The per-column fidelity score  $\varphi(c)$  combines these multiplicatively:

$$\varphi(c) = \varphi_{\text{pres}}(c) \cdot \varphi_{\text{type}}(c) \cdot \varphi_{\text{val}}(c) \quad (13)$$

For *Column Pair Trends*, we compute pairwise similarity on all type-separated columns. Continuous–continuous pairs use Correlation Similarity  $(1 - |r_{\text{real}} - r_{\text{synth}}|/2)$ , discrete–discrete pairs use 2D TV Complement on the joint distribution, and mixed pairs discretize the continuous column into 10 bins, following the widely used SDMetrics implementation. Pairs are weighted by co-occurrence rate  $w(a, b) \propto \max(\text{co\_rate}_{\text{real}}, \text{co\_rate}_{\text{synth}})$ , naturally down-weighting pairs that rarely co-occur due to structural missingness.

*Utility*. ML utility (sometimes referred to as ML efficacy) measures whether synthetic data preserves the predictive structure of the original data. We follow the Train-Synthetic-Test-Real (TSTR) protocol [44]: train a classifier on synthetic data and evaluate on held-out real data, then compare against a baseline model trained on real data (TRTR). All datasets in our benchmark are classification

tasks. The utility score is the ratio of TSTR to TRTR weighted  $F_1$ , capped at 1.0:

$$\text{Utility} = \min\left(\frac{F_1^{\text{TSTR}}}{F_1^{\text{TRTR}}}, 1.0\right) \quad (14)$$

We report both TRTR and TSTR  $F_1$  scores alongside the ratio to allow direct comparison. XGBoost is configured with default hyperparameters ( $n\_estimators=100$ ,  $max\_depth=6$ ) and native categorical support to avoid one-hot explosion on high-cardinality features.

*Detection.* Detection measures whether a classifier can distinguish synthetic records from real ones, following the Classifier Two-Sample Test (C2ST) framework [21]. The standard approach in the tabular synthesis literature uses logistic regression for this test [7], but we observe that the default solver frequently fails to converge within the iteration budget, producing an undertrained classifier that cannot reliably separate real from synthetic data. This artificially inflates detection scores: for example, the results reported in [29] show detection scores in the high 90’s for all competitive methods, providing little discriminative power between synthesizers. We replace logistic regression with an XGBoost classifier ( $n\_estimators=100$ ,  $max\_depth=6$ , native categorical support), which converges reliably and can detect non-linear feature interactions that a linear classifier like logistic regression cannot separate. Stratified 3-fold cross-validation is used to avoid overfitting. Per-fold ROC AUC is clamped to [0.5, 1.0] and transformed:

$$\text{Detection} = 1 - \text{mean}(\max(0.5, \text{AUC}_j) \cdot 2 - 1) \quad (15)$$

where  $\text{AUC}_j$  is the ROC AUC on fold  $j$  of a stratified  $k$ -fold cross-validation. A score of 1.0 means the classifier performs at chance (indistinguishable); 0.0 means perfect separation. We report the raw (unclamped) ROC AUC alongside the detection score for more granular comparison.

*Privacy.* Privacy measures whether the synthesizer memorizes training records. We adopt the Distance to Closest Record (DCR) methodology [19].

For privacy evaluation, we require equally sized reference sets to avoid biasing the DCR toward the larger set. We therefore create a separate 50/50 split from the original training partition, train a new model on one half, and generate an equal number of synthetic records. This yields equally sized train, test, and synthetic sets for distance computation.

For each synthetic record, we compute its  $L_2$  distance to the nearest training record and the nearest test record in the one-hot encoded, range-normalized feature space. If the synthetic data does not memorize training data, it should be equally likely to be closer to either reference set:

$$\text{DCR} = \frac{|\{s \in S : d(s, \text{Train}) < d(s, \text{Test})\}|}{|S|} \cdot 100\% \quad (16)$$

A DCR of 50% is ideal. The privacy score penalizes only values above 50% (closer to train = memorization):

$$\text{Privacy} = 1 - 2 \cdot \max(\text{DCR}/100 - 0.5, 0) \quad (17)$$

We additionally report the number of exact matches (zero-distance pairs) between synthetic and training records as a direct memorization indicator.

For DDXPlus, we report DCR privacy metrics over 3 replicates rather than 10. A single evaluation requires over 12 hours due to the pairwise distance computation over  $580k \times 580k$  records in 6,902 dimensions. The standard error across 3 replicates is sufficiently small to support reliable conclusions.

## 4.5 Model Training Details

We compare ORIGAMI against six baselines covering all different architecture families: TVAE (VAE), CTGAN (GAN), REalTabFormer and TabularARGN (autoregressive), Tabby (LLM), TabDiff (diffusion). We additionally attempted to include GReaT [2] but were unable to obtain results due to sampling failures and architectural limitations, as discussed below.

*TVAE and CTGAN.* We use the SDV [24] library implementation with default hyperparameters (300 epochs) for both models. Both TVAE and CTGAN exceeded the maximum available memory for the Electric Vehicles, Yelp and DDXPlus datasets due to its one-hot encoding of high-cardinality categorical columns. The SDV library itself warns about this: “*PerformanceAlert: Using the CTGANSynthesizer on this data is not recommended*”. We marked the entries for these datasets OOM in the results tables.

*REalTabFormer.* We use the published implementation with default settings. For the Yelp dataset, we had to disable the sensitivity-based early stopping criterion ( $n\_critics=0$ ) due to memory limitations and instead rely on the built-in fallback mechanism using loss convergence. On Electric Vehicles, training was interrupted after 24h at epoch 40. REalTabFormer was unable to train on DDXPlus, even without sensitivity analysis and with reduced batch size (marked OOM in the results table).

*TabDiff.* For Adult, Diabetes, and Electric Vehicles, we train for the default 8,000 epochs with the default batch size of 4,096 and learning rate of  $10^{-3}$ , following the original paper. For Yelp and DDXPlus, we had to reduce the batch size to 1,024 to fit in GPU memory. For those runs, we also adjusted the learning rate to  $5 \cdot 10^{-4}$  (square-root scaling). We also observed loss spikes during training and added gradient clipping at 1.0 to stabilize convergence. We further needed to disable evaluation during training due to the computational cost of sampling (hours for a sample of DDXPlus). On Yelp, TabDiff reached 461 epochs and DDXPlus reached 392 epochs before exceeding the 24h training budget. We sampled from and evaluated the best checkpoint by evaluation loss.

*TabularARGN.* We use the `mostlyai-engine` Python package<sup>4</sup> and default configurations. No issues were observed during training. For DDXPlus, training was interrupted after 24 hours (81 epochs) and the latest checkpoint evaluated.

*GReaT and Tabby.* Both GReaT [2] and its Mixture-of-Experts extension Tabby [6] build on GPT-2 backbones with a fixed context window of 1,024 tokens. For Yelp and DDXPlus, flattened rows exceed this limit (median  $\sim 2,900$  and  $\sim 3,300$  tokens), making these datasets incompatible with GPT-2 family architectures. On the smaller datasets, GReaT trained successfully but its sampling procedure repeatedly failed to produce valid rows; we therefore excluded

<sup>4</sup><https://github.com/mostly-ai/mostlyai-engine>

it from the results. Tabby produced results on Adult only; all other datasets are marked OOM.

*ORIGAMI.* All five datasets use the same model architecture: 8 transformer layers,  $d_{\text{model}} = 64$ ,  $d_{\text{ff}} = 512$ , 4 attention heads and 5 mixture-of-Gaussians components for the continuous head. Training hyperparameters differ slightly across datasets: batch size is 128 for Adult, Diabetes, and Electric Vehicles and 64 for Yelp and DDXPlus; learning rate ranges from  $1 \cdot 10^{-4}$  to  $5 \cdot 10^{-4}$ ; and training runs range from 50 epochs (DDXPlus) to 400 epochs (Adult, Diabetes), selected via validation loss on inner splits. We train the ORIGAMI models with FP16 mixed precision. Key-order shuffling and grammar/schema constraints are enabled for all runs.

## 5 DISCUSSION

Tables 3–6 report all metrics averaged over the replicate sample sets. ORIGAMI achieves the highest fidelity and detection scores across all five datasets (detection is tied with REalTabFormer on Yelp). Utility scores are highest on four of five datasets, with REalTabFormer slightly ahead on Yelp (0.987 vs 0.977). On the dense benchmarks (Adult, Diabetes), margins over the best baselines are moderate. As sparsity increases, the gap widens: on Electric Vehicles (11% sparsity), several baselines already fail to train (TVAE, CTGAN, Tabby) or produce easily detectable output (TabDiff with ROC AUC 0.947). On the semi-structured datasets (Yelp at 38% sparsity, DDXPlus at 35% sparsity), most remaining baselines either exceed available memory or degrade substantially. TabDiff’s fidelity drops from 0.986 on Adult to 0.799 on DDXPlus, and its detection ROC AUC rises to 0.999, indicating near-perfect separability from real data. ORIGAMI maintains high fidelity across the full range (0.993 to 0.963) and remains the hardest to detect on every dataset (tied with REalTabFormer on Yelp). Detection is consistently the most discriminating metric: even where fidelity scores appear competitive, detection reveals differences invisible to marginal and pairwise statistics.

Privacy scores should be interpreted alongside the other metrics, as a model generating random data would achieve near-perfect privacy while failing on fidelity, utility and detection. Except for one outlier, all methods achieve privacy scores above 0.88 with DCR values near the ideal 50%, indicating no systematic memorization. On Electric Vehicles, REalTabFormer’s privacy score drops to 0.42, signalling a potential overfitting issue on the training data. ORIGAMI’s privacy scores are all at or above 0.97. ORIGAMI produces a notable number of exact matches on Electric Vehicles (323 = 0.15%) and DDXPlus (2,816 = 0.27%), and TabularARGN to a lesser degree on DDXPlus (1,043 = 0.1%). However, we observe nearly identical exact match counts against the held-out test set (320 and 2,757, respectively for ORIGAMI), which the model never saw during training.

**Table 2: Training cost comparison on the Yelp dataset.**

Model	Params	Time/Epoch	Epochs	Total
REalTabFormer	59.4M	2,160 sec	40	>24h
TabDiff	25.8M	187 sec	461	>24h
TabularARGN	9.0M	276 sec	82	6.3h
Origami	1.7M	211 sec	150	8.6h

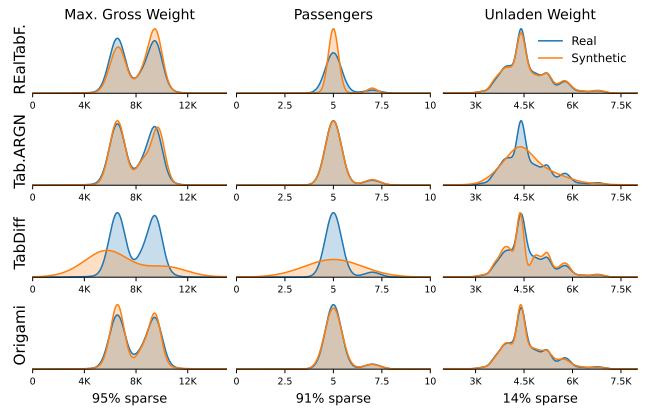


**Figure 4: KDE visualizations of sparse numeric columns on the Electric Vehicles dataset.**

This symmetry indicates that these matches arise from low-entropy records, common attribute combinations that recur throughout the dataset, rather than memorization of training examples.

*Model sizes and training times.* Table 2 compares model sizes and training costs on the Yelp dataset for all models that could successfully train. ORIGAMI is the smallest model by a wide margin at 1.7M parameters, over  $5\times$  smaller than the second-smallest TabularARGN (9.0M) and  $35\times$  smaller than REalTabFormer (59.4M). Both REalTabFormer and TabDiff exceeded the 24-hour training budget. TabularARGN achieves the shortest total training time (6.3h vs. 8.6h for ORIGAMI), which can be attributed to its NADE-inspired MLP architecture that avoids the quadratic attention cost of transformers.

*Preprocessing artifacts in numeric columns.* We further investigate notable outliers in the results by examining the Electric Vehicles dataset, where detection scores start to degrade for TabDiff and TabularARGN. Inspecting the feature importances of the XGBoost detection classifier reveals that the largest contributions come from numeric columns with high rates of structural sparsity: Maximum Gross Weight (95% missing), Passengers (91%), and Unladen Weight (14%). Figure 4 visualizes the kernel density estimates for these columns for all models. For TabDiff, the discrepancy between real and synthetic distributions grows with sparsity: for Maximum Gross Weight and Passengers, TabDiff produces distributions that diverge substantially from the real data. We attribute this to the mean imputation applied during TabDiff’s preprocessing. When 95% of a column’s values are replaced by the column mean before training, the diffusion model learns a distribution dominated by this artificial mode rather than the true conditional distribution of the observed values. This highlights a fundamental limitation of mean imputation for structurally sparse data, where missingness is informative and the observed values follow a distribution far from the column mean.

For TabularARGN, the Unladen Weight column shows visible mismatch despite its low sparsity (14%). TabularARGN encodes this column using quantile-based binning with uniform intra-bin sampling. Further analysis reveals that the sparse tail is covered by a single bin spanning over 71,000 units, replacing a few clustered

**Table 3: Fidelity metrics across datasets (mean  $\pm$  std over 10 replicates). Higher is better, best is underlined.**

		Tabby	TVAE	CTGAN	REaLTabFormer	TabularARGN	TabDiff	ORIGAMI (ours)
Adult	Overall score	0.940 $\pm$ 0.003	0.885 $\pm$ 0.001	0.893 $\pm$ 0.001	0.957 $\pm$ 0.001	0.979 $\pm$ 0.001	0.986 $\pm$ 0.001	<u>0.993</u> $\pm$ 0.000
	Shapes	0.945 $\pm$ 0.001	0.889 $\pm$ 0.001	0.892 $\pm$ 0.001	0.965 $\pm$ 0.001	0.985 $\pm$ 0.001	0.990 $\pm$ 0.001	<u>0.996</u> $\pm$ 0.000
	Trends	0.935 $\pm$ 0.007	0.881 $\pm$ 0.001	0.894 $\pm$ 0.001	0.950 $\pm$ 0.002	0.972 $\pm$ 0.001	0.982 $\pm$ 0.001	<u>0.990</u> $\pm$ 0.001
Diabetes	Overall score	OOM	0.859 $\pm$ 0.000	0.913 $\pm$ 0.000	0.962 $\pm$ 0.000	0.983 $\pm$ 0.000	0.984 $\pm$ 0.000	<u>0.992</u> $\pm$ 0.000
	Shapes	-	0.889 $\pm$ 0.000	0.931 $\pm$ 0.000	0.970 $\pm$ 0.000	0.989 $\pm$ 0.000	0.990 $\pm$ 0.000	<u>0.996</u> $\pm$ 0.000
	Trends	-	0.829 $\pm$ 0.000	0.896 $\pm$ 0.000	0.954 $\pm$ 0.000	0.977 $\pm$ 0.000	0.979 $\pm$ 0.000	<u>0.989</u> $\pm$ 0.000
Electric Vehicles	Overall score	OOM	OOM	OOM	0.864 $\pm$ 0.000	0.968 $\pm$ 0.000	0.973 $\pm$ 0.000	<u>0.975</u> $\pm$ 0.000
	Shapes	-	-	-	0.895 $\pm$ 0.000	0.974 $\pm$ 0.000	0.977 $\pm$ 0.000	<u>0.981</u> $\pm$ 0.000
	Trends	-	-	-	0.832 $\pm$ 0.001	0.962 $\pm$ 0.000	0.968 $\pm$ 0.000	<u>0.969</u> $\pm$ 0.000
Yelp	Overall score	OOM	OOM	OOM	0.911 $\pm$ 0.000	0.883 $\pm$ 0.000	0.865 $\pm$ 0.000	<u>0.963</u> $\pm$ 0.000
	Shapes	-	-	-	0.900 $\pm$ 0.000	0.879 $\pm$ 0.001	0.832 $\pm$ 0.000	<u>0.968</u> $\pm$ 0.000
	Trends	-	-	-	0.922 $\pm$ 0.000	0.886 $\pm$ 0.000	0.898 $\pm$ 0.000	<u>0.958</u> $\pm$ 0.000
DDXPlus	Overall score	OOM	OOM	OOM	OOM	0.790 $\pm$ 0.000	0.799 $\pm$ 0.000	<u>0.972</u> $\pm$ 0.000
	Shapes	-	-	-	-	0.779 $\pm$ 0.000	0.768 $\pm$ 0.000	<u>0.973</u> $\pm$ 0.000
	Trends	-	-	-	-	0.802 $\pm$ 0.000	0.830 $\pm$ 0.000	<u>0.971</u> $\pm$ 0.000

**Table 4: Utility metrics across datasets (mean  $\pm$  std over 10 replicates). Higher is better, best is underlined.**

		Tabby	TVAE	CTGAN	REaLTabFormer	TabularARGN	TabDiff	ORIGAMI (ours)
Adult	Overall score	0.946 $\pm$ 0.003	0.940 $\pm$ 0.003	0.944 $\pm$ 0.004	0.993 $\pm$ 0.001	0.971 $\pm$ 0.003	0.981 $\pm$ 0.002	<u>0.998</u> $\pm$ 0.002
	TRTR $F_1$	0.866 $\pm$ 0.000	0.866 $\pm$ 0.000	0.866 $\pm$ 0.000	0.866 $\pm$ 0.000	0.866 $\pm$ 0.000	0.866 $\pm$ 0.000	<u>0.866</u> $\pm$ 0.000
	TSTR $F_1$	0.820 $\pm$ 0.003	0.814 $\pm$ 0.003	0.817 $\pm$ 0.003	0.860 $\pm$ 0.001	0.841 $\pm$ 0.003	0.850 $\pm$ 0.001	<u>0.864</u> $\pm$ 0.002
Diabetes	Overall score	OOM	0.976 $\pm$ 0.005	0.870 $\pm$ 0.006	0.979 $\pm$ 0.004	0.980 $\pm$ 0.004	0.978 $\pm$ 0.003	<u>0.984</u> $\pm$ 0.004
	TRTR $F_1$	-	0.620 $\pm$ 0.000	0.620 $\pm$ 0.000	0.620 $\pm$ 0.000	0.619 $\pm$ 0.000	0.620 $\pm$ 0.000	<u>0.620</u> $\pm$ 0.000
	TSTR $F_1$	-	0.605 $\pm$ 0.003	0.539 $\pm$ 0.004	0.607 $\pm$ 0.003	0.607 $\pm$ 0.002	0.606 $\pm$ 0.002	<u>0.610</u> $\pm$ 0.002
Electric Vehicles	Overall score	OOM	OOM	OOM	0.869 $\pm$ 0.055	0.978 $\pm$ 0.004	0.946 $\pm$ 0.005	<u>0.991</u> $\pm$ 0.001
	TRTR $F_1$	-	-	-	0.967 $\pm$ 0.000	0.966 $\pm$ 0.000	0.969 $\pm$ 0.000	<u>0.969</u> $\pm$ 0.000
	TSTR $F_1$	-	-	-	0.840 $\pm$ 0.053	0.945 $\pm$ 0.004	0.917 $\pm$ 0.005	<u>0.960</u> $\pm$ 0.001
Yelp	Overall score	OOM	OOM	OOM	<u>0.987</u> $\pm$ 0.002	0.974 $\pm$ 0.002	0.959 $\pm$ 0.002	0.977 $\pm$ 0.004
	TRTR $F_1$	-	-	-	0.844 $\pm$ 0.001	0.844 $\pm$ 0.000	0.845 $\pm$ 0.001	<u>0.844</u> $\pm$ 0.002
	TSTR $F_1$	-	-	-	0.833 $\pm$ 0.002	0.822 $\pm$ 0.002	0.811 $\pm$ 0.002	<u>0.824</u> $\pm$ 0.002
DDXPlus	Overall score	OOM	OOM	OOM	OOM	0.990 $\pm$ 0.003	0.991 $\pm$ 0.001	<u>0.999</u> $\pm$ 0.000
	TRTR $F_1$	-	-	-	-	0.997 $\pm$ 0.003	0.997 $\pm$ 0.000	<u>0.997</u> $\pm$ 0.000
	TSTR $F_1$	-	-	-	-	0.988 $\pm$ 0.002	0.988 $\pm$ 0.001	<u>0.996</u> $\pm$ 0.000

outliers with a uniform fill. In the dense core, the real data concentrates at a small number of exact vehicle weights, but the uniform sampling spreads these peaks across each bin’s range, producing the smoother, flatter distribution visible in Figure 4, again suggesting that numeric discretization can introduce artifacts that a good classifier can pick up on.

*Position Encoding.* To demonstrate the effectiveness of KVPE over sequential position encoding as used in GPT-2, we construct a pathological synthetic dataset of 5,000 nested JSON records with 4 branches (a–d), each containing two sub-objects (left, right) with a single boolean leaf named val, for a total of 8 leaf paths per record that all share common key names:

```

{"a": {"left": {"val": true}, "right": {"val": false}},
 "b": {"left": {"val": false}, "right": {"val": true}},
 "c": {"left": {"val": true}, "right": {"val": false}},
 "d": {"left": {"val": true}, "right": {"val": false}}

```

Each key path has a distinct Bernoulli parameter ranging from 0.05 to 0.95 from which we draw its boolean values across records. Since the key order is shuffled at every nesting level during training, it makes sequential token positions uninformative. We train small ORIGAMI models (2 layers,  $d_{\text{model}}=32$ , 4 heads) for 50 epochs with KVPE and sequential PE respectively, and measure per-path mean absolute error (MAE) of the generated marginals, repeating the training and sampling process across 3 random seeds. Figure 5(a) shows that KVPE achieves consistently lower validation loss. Figure 5(b) confirms the cause: KVPE recovers the true per-path marginals (MAE  $0.042 \pm 0.035$ ), while sequential PE collapses to a uniform  $\approx 0.5$  for all paths (MAE  $0.271 \pm 0.003$ ), unable to disambiguate identically-named leaves at different key paths.

*Key Order Permutations.* ORIGAMI and some other autoregressive methods [2, 35] randomize the order of keys/columns in each record

**Table 5: Detection metrics across datasets (mean  $\pm$  std over 10 replicates). Detection score: higher means harder to detect (better). XGBoost classifier ROC AUC: lower means harder to distinguish from real data (better). Best is underlined.**

		Tabby	TVAE	CTGAN	REaLTabFormer	TabularARGN	TabDiff	ORIGAMI (ours)
Adult	Overall score $\uparrow$	$0.335 \pm 0.003$	$0.068 \pm 0.001$	$0.085 \pm 0.002$	$0.815 \pm 0.004$	$0.733 \pm 0.005$	$0.866 \pm 0.005$	<u><math>0.960 \pm 0.005</math></u>
	ROC AUC $\downarrow$	$0.832 \pm 0.001$	$0.966 \pm 0.001$	$0.958 \pm 0.001$	$0.593 \pm 0.002$	$0.634 \pm 0.002$	$0.567 \pm 0.003$	$0.520 \pm 0.002$
Diabetes	Overall score $\uparrow$	OOM	$0.002 \pm 0.000$	$0.082 \pm 0.002$	$0.666 \pm 0.004$	$0.789 \pm 0.005$	$0.645 \pm 0.006$	<u><math>1.000 \pm 0.000</math></u>
	ROC AUC $\downarrow$	-	$0.999 \pm 0.000$	$0.959 \pm 0.001$	$0.667 \pm 0.002$	$0.606 \pm 0.002$	$0.677 \pm 0.003$	$0.473 \pm 0.002$
Electric Vehicles	Overall score $\uparrow$	OOM	OOM	OOM	<u><math>0.413 \pm 0.001</math></u>	$0.303 \pm 0.004$	$0.106 \pm 0.003$	<u><math>0.413 \pm 0.004</math></u>
	ROC AUC $\downarrow$	-	-	-	$0.794 \pm 0.000$	$0.849 \pm 0.002$	$0.947 \pm 0.002$	$0.794 \pm 0.002$
Yelp	Overall score $\uparrow$	OOM	OOM	OOM	$0.249 \pm 0.001$	$0.118 \pm 0.001$	$0.008 \pm 0.000$	<u><math>0.725 \pm 0.005</math></u>
	ROC AUC $\downarrow$	-	-	-	$0.875 \pm 0.000$	$0.941 \pm 0.001$	$0.996 \pm 0.000$	$0.638 \pm 0.002$
DDXPlus	Overall score $\uparrow$	OOM	OOM	OOM	OOM	$0.062 \pm 0.001$	$0.002 \pm 0.000$	<u><math>0.377 \pm 0.005</math></u>
	ROC AUC $\downarrow$	-	-	-	-	$0.969 \pm 0.000$	$0.999 \pm 0.000$	$0.812 \pm 0.002$

**Table 6: Privacy metrics across datasets (mean  $\pm$  std over 10 replicates, 3 replicates for DDXPlus). Privacy score: higher is better. DCR score  $\leq 50$  indicates no memorization. Best is underlined.**

		Tabby	TVAE	CTGAN	REaLTabFormer	TabularARGN	TabDiff	ORIGAMI (ours)
Adult	Overall score $\uparrow$	<u><math>1.000 \pm 0.000</math></u>	$0.982 \pm 0.009$	$0.988 \pm 0.005$	$0.913 \pm 0.006$	$0.993 \pm 0.006$	$0.882 \pm 0.006$	$0.986 \pm 0.006$
	DCR $\downarrow$	$49.177 \pm 0.325$	$50.914 \pm 0.439$	$50.604 \pm 0.232$	$54.367 \pm 0.319$	$50.349 \pm 0.283$	$55.900 \pm 0.325$	$50.720 \pm 0.311$
	Exact match $\downarrow$	$0.0 \pm 0.0$	$0.0 \pm 0.0$	$0.0 \pm 0.0$	$3.1 \pm 1.4$	$0.0 \pm 0.0$	$0.0 \pm 0.0$	$0.2 \pm 0.4$
Diabetes	Overall score $\uparrow$	OOM	$0.974 \pm 0.005$	<u><math>1.000 \pm 0.000</math></u>	$0.882 \pm 0.001$	$0.969 \pm 0.004$	$0.945 \pm 0.005$	$0.969 \pm 0.004$
	DCR $\downarrow$	-	$51.309 \pm 0.259$	$49.678 \pm 0.238$	$55.908 \pm 0.071$	$51.528 \pm 0.205$	$52.746 \pm 0.241$	$51.544 \pm 0.198$
	Exact match $\downarrow$	-	$0.0 \pm 0.0$	$0.0 \pm 0.0$	$0.4 \pm 0.5$	$0.0 \pm 0.0$	$0.1 \pm 0.3$	$0.1 \pm 0.3$
Electric Vehicles	Overall score $\uparrow$	OOM	OOM	OOM	$0.417 \pm 0.003$	$0.998 \pm 0.002$	$0.953 \pm 0.002$	<u><math>1.000 \pm 0.000</math></u>
	DCR $\downarrow$	-	-	-	$79.172 \pm 0.141$	$50.048 \pm 0.135$	$52.373 \pm 0.124$	$49.489 \pm 0.113$
	Exact match $\downarrow$	-	-	-	$0.0 \pm 0.0$	$0.0 \pm 0.0$	$0.0 \pm 0.0$	$333.3 \pm 17.9$
Yelp	Overall score $\uparrow$	OOM	OOM	OOM	$0.909 \pm 0.006$	$0.959 \pm 0.003$	<u><math>0.994 \pm 0.003</math></u>	$0.973 \pm 0.002$
	DCR $\downarrow$	-	-	-	$54.549 \pm 0.281$	$52.034 \pm 0.142$	$50.310 \pm 0.169$	$51.328 \pm 0.107$
	Exact match $\downarrow$	-	-	-	$0.0 \pm 0.0$	$0.0 \pm 0.0$	$0.0 \pm 0.0$	$0.0 \pm 0.0$
DDXPlus	Overall score $\uparrow$	OOM	OOM	OOM	OOM	<u><math>1.000 \pm 0.000</math></u>	$0.984 \pm 0.001$	<u><math>1.000 \pm 0.000</math></u>
	DCR $\downarrow$	-	-	-	-	$49.785 \pm 0.050$	$50.815 \pm 0.056$	$49.728 \pm 0.034$
	Exact match $\downarrow$	-	-	-	-	$1043.0 \pm 42.6$	$0.0 \pm 0.0$	$2851.8 \pm 29.9$

at every training step. We hypothesize that this prevents the model from exploiting key ordering as a spurious feature, forcing it to learn the actual statistical relationships between values.

We ablate this on the Adult dataset by training two identical models for 200 epochs: one with key shuffling enabled and one without. Table 7 reports the results. Without shuffling, the model achieves marginally higher fidelity (0.993 vs. 0.991), as it converges more tightly to the training distribution. Perhaps counter-intuitively, this tighter fit does not translate into higher utility. The shuffled model achieves a notably higher utility score (0.998 vs. 0.992), with TSTR  $F_1$  improving from 0.859 to 0.864. The tighter fit of the unshuffled model also comes at a steep privacy cost: the DCR increases to 72.8% (vs. 55.1% with shuffling), and 91 synthetic records are exact copies of training examples compared to just 1 with shuffling enabled. The training curves (Figure 6) corroborate this: without shuffling, the validation loss begins to diverge from the training loss after epoch 25 and rises steadily (a classic overfitting signature). With shuffling, both losses decrease together and the validation

loss remains stable. The higher loss baseline for shuffled training runs can be attributed to the unpredictable key token order.

These results confirm that key shuffling, combined with an order-invariant position encoding, acts as an effective data augmentation strategy. By presenting each record in a random key order, it increases the effective training set size without requiring additional data, preventing memorization while preserving the model’s ability to capture the underlying data distribution.

*Key Takeaways.* Our experiments reveal several practical lessons for synthesizing sparse, semi-structured data. First, one-hot encoding of categoricals does not scale and should be avoided due to the column explosion on high-cardinality categorical columns, even during preprocessing of the data. This problem compounds on semi-structured data: flattening nested structures turns array elements into separate columns like `categories.0`, `categories.1`, `categories.2`, ... with identical category sets, multiplying the encoded dimensionality. This quickly exceeds available memory (as seen with CTGAN and TVAE on Electric Vehicles, Yelp and

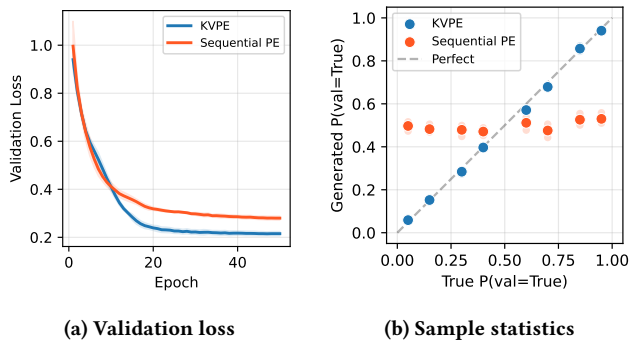


**Figure 5: KVPE vs. sequential position encoding on a synthetic nested JSON dataset. KVPE accurately recovers path-specific marginals while sequential PE collapses to uniform ( $\approx 0.5$ ). Results over 3 seeds.**

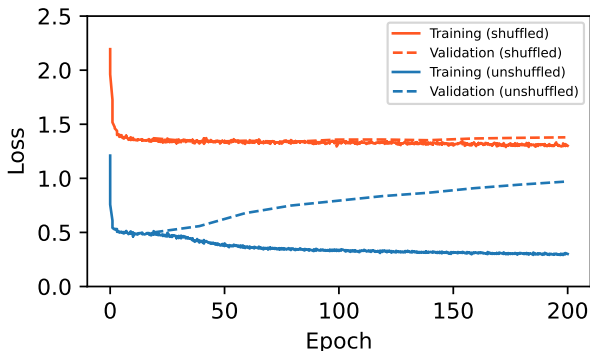


**Figure 6: Loss curves on Adult with/ without key shuffling.**

**Table 7: Ablation of key-order shuffling on the Adult dataset.**

	No Shuffling	Shuffling
Fidelity	<b>0.993</b>	0.991
Column Shapes	0.996	0.994
Column Trends	0.990	0.988
Utility	0.992	<b>0.998</b>
TSTR $F_1$	0.859	0.864
TRTR $F_1$	0.866	0.866
Privacy	0.544	<b>0.897</b>
DCR (%)	72.8	55.1
Exact matches	91	1

DDXPlus). A more scalable alternative is to map each category to a dense vector via a learned embedding matrix, which keeps memory constant regardless of cardinality and allows the representations to be refined during training. Handling sparsity also requires care. For categoricals, adding a sentinel value like “\_missing\_” works well enough, as it only adds one extra category per column, as long as the post-processor removes these values from the final output. For numerics, imputation is more problematic: when the majority of

values in a column are replaced by its mean, the model learns a distribution dominated by this artificial mode rather than the true distribution of observed values, producing output that is easy to tell apart from real data (Figure 4, TabDiff). Similarly, discretizing numeric values through binning or per-digit encoding introduces artifacts that a strong classifier detects; modeling numerics in continuous space with a hybrid architecture avoids this problem. Our results also show that autoregressive models are competitive with diffusion-based approaches, but the choice of backbone and tokenizer matters. Standard language model architectures with subword tokenizers (GReaT, Tabby) inherit a large fixed vocabulary and a limited context window, both of which become bottlenecks on wide or semi-structured datasets. Dataset-specific vocabularies, as used in REaLTabFormer and adopted in ORIGAMI, address this by including only the keys and values observed in the training data, producing shorter token sequences that scale to hundreds of columns. Beyond efficiency, a structured vocabulary with explicit token classes for keys, values, and structural delimiters enables grammar and schema constraints that would be difficult to enforce over free-form subword tokens. Finally, randomly permuting the key order during training acts as an effective regularizer against overfitting and memorization, reducing exact training-set copies while maintaining comparable fidelity and utility.

## 6 CONCLUSION

We presented ORIGAMI, an autoregressive transformer that synthesizes data directly from tokenized JSON records, avoiding the flattening and imputation steps that existing tabular methods require. By combining Key-Value Position Encoding with key-order shuffling, a dual-head discrete/continuous architecture, and grammar and schema constraints enforced via a pushdown automaton, ORIGAMI natively handles the nested objects, variable-length arrays, sparsity, and type polymorphism found in semi-structured data.

On dense tabular benchmarks, ORIGAMI matches or exceeds state-of-the-art baselines across fidelity, utility, and detection metrics. As datasets grow sparser and more structured, the gap widens: most baselines either exhaust available memory or produce output that is easily distinguished from real data, while ORIGAMI maintains high-quality synthesis across all settings.

Several directions remain open. Extending the architecture to multi-collection relational data, where foreign-key dependencies introduce cross-record structure, is a natural next step. More broadly, as an autoregressive model, ORIGAMI is a tractable density estimator over semi-structured data, providing direct access to likelihood estimates. This opens applications beyond synthetic data generation: conditional sampling and data imputation (by fixing a subset of keys and generating the rest), cardinality estimation for query optimization—extending work on learned cardinality estimators for relational tables [43] to semi-structured data—predictive modeling over semi-structured records, and outlier detection via low-likelihood scoring.

## REFERENCES

- [1] Michael A. Alcorn and Anh Nguyen. 2021. The DEformer: An Order-Agnostic Distribution Estimating Transformer. <http://arxiv.org/abs/2106.06989>
- [2] Vadim Borisov, Kathrin Seßler, Tobias Leemann, Martin Pawelczyk, and Gjergji Kasneci. 2023. Language Models are Realistic Tabular Data Generators. In *International Conference on Learning Representations (ICLR)*.

- [3] Pierre Bourhis, Juan L. Reutter, Fernando Suárez, and Domagoj Vrgoč. 2017. JSON: Data Model, Query Languages and Schema Specification. In *Proceedings of the 36th ACM SIGMOD-SIGACT-SIGAI Symposium on Principles of Database Systems (PODS)*. 123–135. <https://doi.org/10.1145/3034786.3056120>
- [4] Kuntai Cai, Xiaokui Xiao, and Graham Cormode. 2023. PrivLava: Synthesizing Relational Data with Foreign Keys under Differential Privacy. In *Proceedings of the 2023 International Conference on Management of Data*. ACM, 1–25.
- [5] Michael Carey, Wail Alkawaileet, Nick DiGeronimo, Peeyush Gupta, Sachin Smotra, and Till Westmann. 2025. Towards Principled, Practical Document Database Design. *Proceedings of the VLDB Endowment* 18, 12 (2025), 4804–4816. <https://doi.org/10.14778/3750601.3750606>
- [6] Sonia Crompt, Satya Sai Srinath Namburi GNVV, Mohammed Alkhudhayri, Catherine Cao, Samuel Guo, Nicholas Roberts, and Frederic Sala. 2026. Tabby: A Language Model Architecture for Tabular and Structured Data Synthesis. *Transactions on Machine Learning Research* (2026). <https://openreview.net/forum?id=b9FPVnb0Bn>
- [7] DataCebo, Inc. 2026. *Synthetic Data Metrics*. DataCebo, Inc. <https://docs.sdv.dev/sdmetrics/> Version 0.12.0.
- [8] Arsene Fansi Tchango, Rishab Goel, Zhi Wen, Julien Martel, and Joumana Ghosn. 2022. DDXPlus: A New Dataset for Automatic Medical Diagnosis. In *Advances in Neural Information Processing Systems*, Vol. 35. 31306–31318.
- [9] Philip Gage. 1994. A new algorithm for data compression. *C Users J*, 12, 2 (Feb. 1994), 23–38.
- [10] Yunqing Ge et al. 2025. Privacy-Enhanced Database Synthesis for Benchmark Publishing. *Proceedings of the VLDB Endowment* 18, 2 (2025).
- [11] Siavash Golkar, Mariel Pettee, Michael Eickenberg, Alberto Bietti, Miles Cranmer, Geraud Kraewzik, Francois Lanusse, Michael McCabe, Ruben Ohana, Liam Parker, Bruno Régalo-Saint Blancard, Tiberiu Tesileanu, Kyunghyun Cho, and Shirley Ho. 2023. xVal: A Continuous Number Encoding for Large Language Models. <http://arxiv.org/abs/2310.02989>
- [12] Ian J. Goodfellow, Jean Pouget-Abadie, Mehdi Mirza, Bing Xu, David Warde-Farley, Sherjil Ozair, Aaron Courville, and Yoshua Bengio. 2014. Generative Adversarial Networks. In *Advances in Neural Information Processing Systems*, Vol. 27.
- [13] Dan Hendrycks and Kevin Gimpel. 2016. Gaussian Error Linear Units (GELUs). <http://arxiv.org/abs/1606.08415>
- [14] James Jordon, Lukasz Szpruch, Florimond Houssiau, Mirko Bottarelli, Giovanni Cherubin, Carsten Maple, Samuel N. Cohen, and Adrian Weller. 2022. Synthetic Data – What, Why and How? <http://arxiv.org/abs/2205.03257>
- [15] Markelle Kelly, Rachel Longjohn, and Kolby Nottingham. [n.d.]. The UCI Machine Learning Repository. <https://archive.ics.uci.edu>
- [16] Diederik P. Kingma and Max Welling. 2014. Auto-Encoding Variational Bayes. In *International Conference on Learning Representations (ICLR)*.
- [17] Terry Koo, Frederick Liu, and Luheng He. 2024. Automata-Based Constraints for Language Model Decoding. In *Conference on Language Modeling*. <https://openreview.net/forum?id=BDBdblmlyZ>
- [18] Akim Kotelnikov, Dmitry Baranchuk, Ivan Rubachev, and Artem Babenko. 2023. TabDDPM: Modelling Tabular Data with Diffusion Models. In *International Conference on Machine Learning (ICML)*. 17564–17579.
- [19] Qinyi Liu, Mohammad Khalil, Jelena Jovanovic, and Ronas Shakya. 2024. Scaling While Privacy Preserving: A Comprehensive Synthetic Tabular Data Generation and Evaluation in Learning Analytics. In *Proceedings of the 14th Learning Analytics and Knowledge Conference (LAK)*. 620–631. <https://doi.org/10.1145/3636555.3636921>
- [20] Tension Liu, Zhaozhi Qian, Jeroen Berrevoets, and Mihaela van der Schaar. 2023. GOGGLE: Generative Modelling for Tabular Data by Learning Relational Structure. In *International Conference on Learning Representations (ICLR)*.
- [21] David Lopez-Paz and Maxime Oquab. 2017. Revisiting Classifier Two-Sample Tests. In *International Conference on Learning Representations (ICLR)*.
- [22] Shubhankar Mohapatra, Jianqiao Zong, Florian Kerschbaum, and Xi He. 2024. Differentially Private Data Generation with Missing Data. *Proceedings of the VLDB Endowment* 17, 8 (2024), 2022–2035.
- [23] Phil Ostheimer, Mayank Nagda, Andriy Balinsky, Jean Radig, Carl Herrmann, Stephan Mandt, Marius Kloft, and Sophie Fellenz. 2025. Sparse Data Diffusion for Scientific Simulations in Biology and Physics. *arXiv preprint arXiv:2502.02448* (2025).
- [24] Neha Patki, Roy Wedge, and Kalyan Veeramachaneni. 2016. The Synthetic Data Vault. In *2016 IEEE International Conference on Data Science and Advanced Analytics (DSAA)*. 399–410. <https://doi.org/10.1109/DSAA.2016.49>
- [25] F. Pedregosa, G. Varoquaux, A. Gramfort, V. Michel, B. Thirion, O. Grisel, M. Blondel, P. Prettenhofer, R. Weiss, V. Dubourg, J. Vanderplas, A. Passos, D. Cournapeau, M. Brucher, M. Perrot, and E. Duchesnay. 2011. Scikit-learn: Machine learning in Python. *Journal of Machine Learning Research* 12 (2011), 2825–2830.
- [26] Felipe Pezoa, Juan L. Reutter, Fernando Suarez, Martin Ugarte, and Domagoj Vrgoč. 2016. Foundations of JSON schema. In *Proceedings of the 25th international conference on world wide web (WWW)*. 263–273.
- [27] Alec Radford, Karthik Narasimhan, Tim Salimans, and Ilya Sutskever. 2018. Improving Language Understanding by Generative Pre-Training. [https://cdn.openai.com/research-covers/language-unsupervised/language\\_understanding\\_paper.pdf](https://cdn.openai.com/research-covers/language-unsupervised/language_understanding_paper.pdf)
- [28] Tobias Schmidt, Viktor Leis, Peter Boncz, and Thomas Neumann. 2025. SQLStorm: Taking Database Benchmarking into the LLM Era. *Proceedings of the VLDB Endowment* 18, 11 (2025), 4144–4157. <https://doi.org/10.14778/3749646.3749683>
- [29] Juntong Shi, Minkai Xu, Harper Hua, Hengrui Zhang, Stefano Ermon, and Jure Leskovec. 2025. TabDiff: a Mixed-type Diffusion Model for Tabular Data Generation. In *The Thirteenth International Conference on Learning Representations*. <https://openreview.net/forum?id=swvURjrt8z>
- [30] Ruxue Shi, Yili Wang, Mengnan Du, Xu Shen, Yi Chang, and Xin Wang. 2025. A Comprehensive Survey of Synthetic Tabular Data Generation. <http://arxiv.org/abs/2504.16506>
- [31] Aivin V. Solatorio and Olivier Dupriez. 2023. REalTabFormer: Generating Realistic Relational and Tabular Data using Transformers. <http://arxiv.org/abs/2302.02041>
- [32] Nitish Srivastava, Geoffrey Hinton, Alex Krizhevsky, Ilya Sutskever, and Ruslan Salakhutdinov. 2014. Dropout: A Simple Way to Prevent Neural Networks from Overfitting. *Journal of Machine Learning Research* 15, 56 (2014), 1929–1958.
- [33] Michael Stonebraker and Andrew Pavlo. 2024. What Goes Around Comes Around... And Around... *ACM Sigmod Record* 53, 2 (2024), 21–37.
- [34] Jianlin Su, Murtdha Ahmed, Yu Lu, Shengfeng Pan, Wen Bo, and Yunfeng Liu. 2024. RoFormer: Enhanced Transformer with Rotary Position Embedding. *Neurocomputing* 568 (2024), 127063. <https://doi.org/10.1016/j.neucom.2023.127063>
- [35] Paul Tiwald, Ivona Krchova, Andrey Sidorenko, Mariana Vargas Vieyra, Mario Scriminaci, and Michael Platzer. 2025. TabularARGN: A Flexible and Efficient Auto-Regressive Framework for Generating High-Fidelity Synthetic Data. <http://arxiv.org/abs/2501.12012>
- [36] Benigno Uribe, Iain Murray, and Hugo Larochelle. 2014. A Deep and Tractable Density Estimator. In *International Conference on Machine Learning (ICML)*. 467–475.
- [37] Ashish Vaswani, Noam Shazeer, Niki Parmar, Jakob Uszkoreit, Llion Jones, Aidan N. Gomez, Łukasz Kaiser, and Illia Polosukhin. 2017. Attention is All You Need. In *Advances in Neural Information Processing Systems*, Vol. 30. 5998–6008.
- [38] Brandon T. Willard and Rémi Louf. 2023. Efficient Guided Generation for Large Language Models. <http://arxiv.org/abs/2307.09702> arXiv:2307.09702 [cs]
- [39] Yonghui Wu, Mike Schuster, Zhifeng Chen, Quoc V. Le, Mohammad Norouzi, Wolfgang Macherey, Maxim Krikun, Yuan Cao, Qin Gao, Klaus Macherey, Jeff Klingner, Apurva Shah, Melvin Johnson, Xiaobing Liu, Lukasz Kaiser, Stephan Gouws, Yoshikiyo Kato, Taku Kudo, Hideto Kazawa, Keith Stevens, George Kurian, Nishant Patil, Wei Wang, Cliff Young, Jason Smith, Jason Riesa, Alex Rudnick, Oriol Vinyals, Greg Corrado, Macduff Hughes, and Jeffrey Dean. 2016. Google’s Neural Machine Translation System: Bridging the Gap between Human and Machine Translation. <http://arxiv.org/abs/1609.08144>
- [40] Lei Xu, Maria Skoularidou, Alfredo Cuesta-Infante, and Kalyan Veeramachaneni. 2019. Modeling Tabular Data using Conditional GAN. In *Advances in Neural Information Processing Systems*, Vol. 32.
- [41] Jingyi Yang, Peizhi Wu, Gao Cong, Tong Yang, and Jianfei Ruan. 2022. SAM: Database Generation from Query Workloads with Supervised Autoregressive Models. In *Proceedings of the 2022 International Conference on Management of Data*. ACM, 1542–1555.
- [42] Zhilin Yang, Zihang Dai, Yiming Yang, Jaime Carbonell, Ruslan Salakhutdinov, and Quoc V. Le. 2019. XLNet: Generalized Autoregressive Pretraining for Language Understanding. In *Advances in Neural Information Processing Systems*, Vol. 32.
- [43] Zongheng Yang, Eric Liang, Amogh Kamsetty, Chenggang Wu, Yan Duan, Xi Chen, Pieter Abbeel, Joseph M. Hellerstein, Sanjay Krishnan, and Ion Stoica. 2019. Deep Unsupervised Cardinality Estimation. *Proceedings of the VLDB Endowment* 13, 3 (2019), 279–292. <https://doi.org/10.14778/3368289.3368294>
- [44] Yefeng Yuan, Yuhong Liu, and Liang Cheng. 2025. A Multi-Faceted Evaluation Framework for Assessing Synthetic Data Generated by Large Language Models. <http://arxiv.org/abs/2404.14445>
- [45] Hengrui Zhang, Jiani Zhang, Balasubramanian Srinivasan, Zhengyuan Shen, Xiao Qin, Christos Faloutsos, Huzefa Rangwala, and George Karypis. 2024. Mixed-Type Tabular Data Synthesis with Score-based Diffusion in Latent Space. In *International Conference on Learning Representations (ICLR)*.